



Development of a Matrix-Based Bi-Orthogonal FBMC-OQAM Data Model Using Hadamard Scheme

Mahmud J., Tekanyi, A. M. S., Sani, S. M.

Department of Electronics and Telecommunications Engineering,
Ahmadu Bello University Zaria

ABSTRACT

Filter Bank Multicarrier (FBMC) is an OFDM based multicarrier scheme that employs the use of prototype filter in place of cyclic prefix to nullify inter-carrier interference and inter-symbol interference and is suitable for time and frequency localization. As a result, the spectral efficiency of FBMC is higher than other OFDM-based multicarrier techniques that use cyclic prefix. By modulating FBMC complex data symbols using offset quadrature amplitude modulation technique, capacity gain was improved but at the expense of disorienting the orthogonality of the imaginary components of the complex data symbols. This however, was corrected using Hadamard error correction coding scheme in order to obtain OQAM-modulated FBMC symbols which are orthogonal in both the real and imaginary field of the complex data symbols. The developed data symbols were represented in matrix format in order to simplify the computation involved.

ARTICLE INFO

Article History

Received: January, 2020

Received in revised form: March, 2020

Accepted: March, 2020

Published online: April, 2020

KEYWORDS

FFT, Filter-bank multicarrier, FBMC-OQAM, Hadamard scheme, IFFT, OOBE, MIMO, multicarrier modulation, PHYDYAS Filter, OFDM.

INTRODUCTION

There is a huge requirement for an effective data transmission in wireless communication systems in present times and in the future. To achieve that, there is need to optimally utilizing both the real and imaginary carrier components of a complex data symbols [1]. Filter Bank Multicarrier Offset Quadrature Amplitude Modulation (FBMC-OQAM) which is based on OFDM, offers higher data and is more spectrally efficient because of its little out of bound emissions (OOBE)[2]. The functionality rationale of FBMC-OQAM is in such a way that the modulation of the subcarriers is done at a shift (offset) of half the symbol period between the imaginary and real components of a complex QAM symbol [3]. Thus, OQAM modulating an FBMC complex data symbol improves the level of capacity gain without occupying additional radio spectrum in the frequency range[4], and it is

also robust to multipath fading [5]. This however come at the expense of disorienting the orthogonality of the imaginary components[2]. The disoriented orthogonality can be set straight by employing Hadamard error correction coding scheme [6]. FBMC-OQAM is primarily similar to FBMC with Cosine-modulated Multi-Time (FBMC-CMT), FBMC with Staggered Multi-Time (FBMC-SMT) and FBMC with Pulse Amplitude Modulation (FBMC-PAM) due to their similar functionality [7]. With these superior advantages, OQAM-modulated FBMC is applicable in the present wireless communication systems and beyond [8]. When transmitting OQAM-modulated data symbols over MIMO system, Imaginary intrinsic interference which is caused by the overlap of the filter response of two adjacent sub-channels is much [9]. Hadamard scheme in the process of restoring complex orthogonality in the imaginary domain, mitigates the effect



of intrinsic imaginary interference by spreading symbols in time and frequency [10]. This research employed Hadamard technique in order to develop a matrix based bi-orthogonal FBMC-OQAM data model.

MULTICARRIER MODULATION

Multicarrier modulation is a modulation technique whereby data signal is split into various parts with a view for transmission over distinct carrier signals of narrow bandwidth [11]. To some degree, multicarrier modulation is resistive of multipath fading, Inter-Symbol Interference

(ISI), and noise [11]. The model equation of a time continuous multicarrier signal [12] is as follows:

$$x(t) = \sum_{k=1}^K \sum_{l=1}^L g_{l,k}(t) x_{l,k} \quad (1)$$

Among the key multicarrier modulation techniques, FBMC-OQAM is more spectrally efficiency and has a better performance in terms of symbol density, time localization, frequency localization, and bi-orthogonality as given in Table 1[9]

Table 1: Comparison of Different Multicarrier Modulation Techniques [9]

Schemes	Maximum Symbol Density	Time Localization	Frequency Localization	Bi-Orthogonality	Independent transmit Symbols
OFDM (without CP)	Yes	Yes	no	Yes	yes
Windowed/Filtered OFDM	No	Yes	yes	Yes	yes
FBMC-QAM	No	Yes	yes	Yes	yes
FBMC-OQAM	Yes	yes	yes	Real only	Yes
Block Spread FBMC-OQAM	Yes	yes	Yes,	Yes, after de-spreading	no

Multipath Propagation

In any wireless communication system, multipath propagation which is caused by atmospheric phenomena, is one in which a radio signal from a transmitter disperses and propagates via multiple channels in order to reach the transmitter[9]. The direct signal has the highest strength at the receiving antenna while the indirect signal have lesser strengths and their model equations are as follows [9]:

$$x_D(t) = \cos(\tilde{S}_0 t) \quad (2)$$

$$x_{R,N}(t) = \dots_n \cos(\tilde{S}_0 t - \tilde{S}_0 \ddagger) \quad (3)$$

where, $x_D(t)$ is the direct signal, $x_{R,N}(t)$ is any n^{th} reflected (indirect) signal, \tilde{S}_0 is angular frequency, \dots_n is the differential amplitude, \ddagger is the differential time.

The transmitter receives a summation of all the propagated signal components, $y(t)$ [9]:

$$y(t) = \sum_{n=0}^{N-1} \dots_n e^{j\omega_n} x(t - \ddagger_n) \quad (4)$$

where, $e^{j\omega_n}$ is a complex exponential component of the amplitude.

A. Offset Quadrature Amplitude Modulated Filter-Bank Multicarrier (FBMC-OQAM)

FBMC employs prototype filter to palliate inter-carrier interference and inter-symbol interference. The prototype filter makes time and frequency localization easier and effective, hence giving FBMC higher

spectral efficiency. OQAM modulation of FBMC is in such a way that the modulation of the subcarriers is done at a shift (offset) of half the symbol period between the imaginary and real components of a complex QAM symbol [3]. The block diagram of FBMC-OQAM data symbol transceiver is shown in figure 1 [9]:

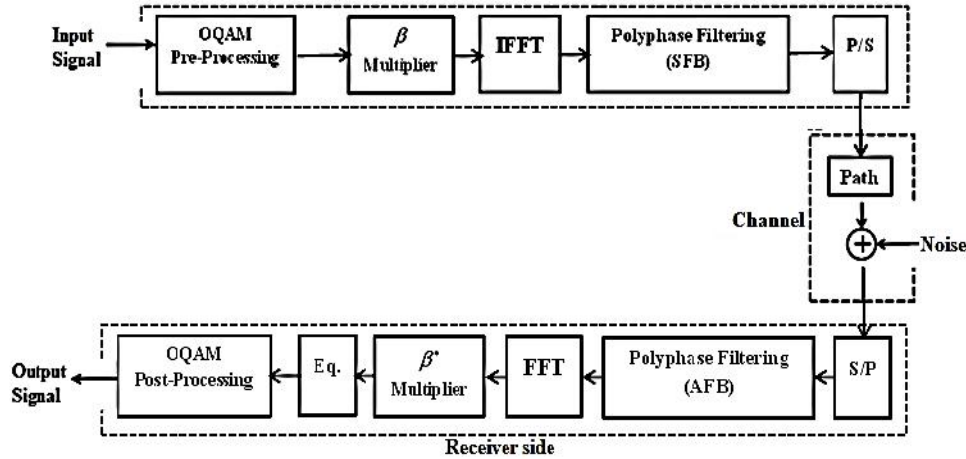


Figure 1: Block Diagram of FBMC-OQAM Transceiver[9].

The model equation of the transmit signal of OQAM-modulated FBMC is given [13] as:

$$s(t) = \sum_{l=0}^{2L+1} \sum_{k=0}^{\infty} d_{l,k} p_{l,k}(t) \quad (5)$$

with,

$$p_{l,k}(t) = j^{l+k} p(t - kT/2) e^{j2\pi f_l t} \quad (6)$$

where, $p_{l,k}(t)$ is the OQAM-modulated prototype pulse and $d_{l,k}$ is the complex OQAM symbol at subcarrier index l and multicarrier index k .

HADAMARD SCHEME

Hadamard coding scheme is a coding scheme whereby the rows of a Hadamard matrix constitute the codewords [14]. Hadamard matrix is a square matrix which has only 1's and -1's arranged in such a way that each row of the matrix is different from other

rows in exactly $N/2$ places, making all the rows to have exactly $N/2$ 1's and $N/2$ -1's, except for a one of the rows that is composed of completely -1's [15]. In a Hadamard matrix, all the rows and columns are mutually orthogonal. Hadamard matrix H of n order (size $n \times n$) is generally presented as follows [16]:

$$HH^* = nI_n \quad (7)$$

where I_n is an identity matrix of size n and H^* is the complex conjugate of H .

The length of the matrix (n) is analogous to the code length. Perfection of the orthogonality comes with the lack of cross correlation between codes. A simple 4×4 Hadamard matrix is as follows [9]:

Corresponding author: Mahmud, J. ✉ mjaysani009@gmail.com ✉ Department of Electronics and Telecommunications Engineering, Ahmadu Bello University, Zaria. © 2020. Faculty of Technology Education, ATBU Bauchi. All rights reserved

$$H_4 = \begin{pmatrix} 1 & 1 & 1 & 1 \\ 1 & -1 & 1 & -1 \\ 1 & 1 & -1 & -1 \\ 1 & -1 & -1 & 1 \end{pmatrix} \quad (8)$$

DEVELOPMENT AND SIMULATION OF FBMC-OQAM DATA MODEL

Considering a Raleigh fading channel, the multicarrier signal source of equation 4 was used to develop an FBMC-OQAM data model. The development was carried out in two steps, first by developing a matrix based FBMC-OQAM data system model and then employing Hadamard coding scheme to the data symbols in order to restore bi-orthogonality.

Development of a Matrix Based FBMC/OQAM Data Model

FBMC/OQAM signal model was developed by constructing and modulating a multicarrier signal in a multipath Raleigh fading channel. The OQAM-modulated FBMC multipath signal was then transformed into a matrix notation by means of computation. It was so transformed into matrix in order to simplify the complex continuous-time multicarrier signal model. The step-by-step

operations for developing the matrix based FBMC-OQAM data model are as follows:

Generating and Simulating the Multipath Signal

The direct ray from a signal source of equation (2) and indirect rays of equation (3) in a multipath fading channel, sum up to give the model equation (4). If the differential time between the direct ray, $x_D(t)$ and the n^{th} reflected ray, $x_{R,N}(t)$ is trifling, and assuming the phase shift of zero, the resultant signal of equation 2.3 will be modeled as the summation of the cosine function as follows:

$$y = \dots \cos(2\pi ft) \quad (9)$$

With the following arbitrary simulation set-up assumptions:

- 64 sample points of the multicarrier signal.
- Maximum propagation time, $t_{\max} = 2e^{-3}$ seconds
- Minimum propagation time, $t_{\min} = 0$ seconds.
- Constant amplitude of one (1).

The received signal was constructed using equation 9 and plotted as presented in figure 2:

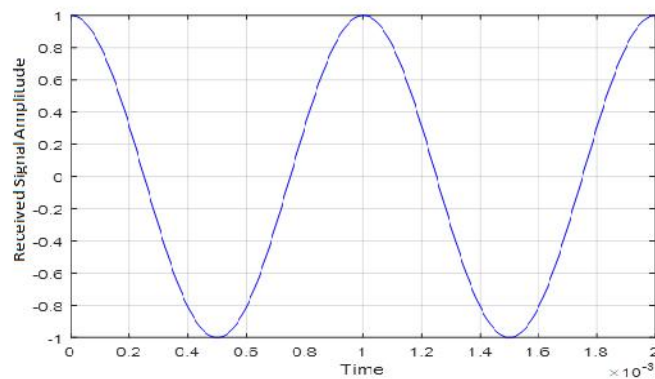


Figure 2: Continuous-Time Multipath Signal

The multicarrier (FBMC) signal was modulated so as to transmit and receive offset QAM symbols, hence the FBMC-OQAM symbols. The tasks carried out in the design of the FBMC signal model are as follows:



QAM Preprocessing

In designing the FBMC-OQAM signal model, complex multipath signal with real and imaginary components was preprocessed and sampled for the offset quadrature amplitude modulation. The sampling set-up parameters and their values are presented in Table 3.1.

IFFT and FFT Design and Implementation

Inverse fast Fourier transform (IFFT) and fast Fourier transform were performed at the transmitter and receiver to conversely convert the multicarrier signal from time domain to frequency domain respectively. The number of data samples $g_i(kK)$ injected to the IFFT input is equal to the number of multicarrier symbols, K . For a range $0 \leq i \leq K - 1$ the resulting IFFT output signal $x[n]$ in the frequency domain was serialized

by parallel-to-serial (P/S) converter and is given as follows [17]:

$$x(n) = \sum_{i=0}^{K-1} g_i(kK) e^{j2f \frac{i(n-kK)}{K}} \quad (10)$$

where k is the symbol index.

The IFFT and FFT were implemented using the following set-up:

Sampling frequency of unity.

Carrier frequency spacing of $1/K$.

Multicarrier symbol period of $T = 1/T_0$.

At the receiver end, a serial-to-parallel (S/P) converter parallelized the signal which was then retrieved from the output of the FFT as follows [17]:

$$g_i(kK) = \frac{1}{K} \sum_{n=kK}^{kK+K-1} x(n) e^{-j2f \frac{i(n-kK)}{K}} \quad (11)$$

Table 3.1: The OQAM Preprocessing Setup Parameters.

S/N	Parameter	Numerical Value	Comment
1	Subcarriers (L)	24	Number of subcarriers for each symbol in FBMC
2	Symbols (K)	64	Large number for better resolution. Precisely 64 in favor of Large MIMO
3	Simulation Iteration	200	Any number will do
4	Subcarrier Spacing (F)	15e3 (Hz)	LTE subcarrier spacing
5	Sampling Rate	15e3 * L * 14 (S/s)	Over sampled by 14 which correspond to CP length of OFDM to monitor OOB

Filter Design and Implementation

The spectral superiority of FBMC comes with the proper design of filter and how they are applied to the subcarriers. The choice of the filter to be used was informed by the energy concentration in time domain, rapid decaying in the frequency domain to reduce Inter-carrier interference (ICI), and flexibility with respect to overlapping factor, R . The

overlapping factor determines the filter length

L_p as shown in equation (3.4) [17]:

$$L_p = RK - 1 \quad (12)$$

Where K is the number of subcarrier symbols.

The computation involved in the design and implementation of PHYDYAS filter is less compared to Hermit filter which was

used by authors such as [18]. This is because PHYDYAS filter maintains the FFT and IFFT sizes of the system.

The continuous frequency response $H(f)$ of the PHYDYAS filter is presented in equation (13) and the impulse response $h(t)$ was derived by taking the IFFT of $H(f)$ and is given in equation (14) [7] and were used in designing the filter:

$$H(f) = \sum_{r=-R}^{R-1} H_r \frac{\sin(f - \frac{r}{RK})RK}{RK \sin(f - \frac{r}{RK})RK} \quad (13)$$

$$h(t) = 1 + 2 \sum_{r=1}^{R-1} H_r \cos(2f \frac{rt}{RT}) \quad (14)$$

The frequency impulse response of the filter is presented in Figure (3.4).

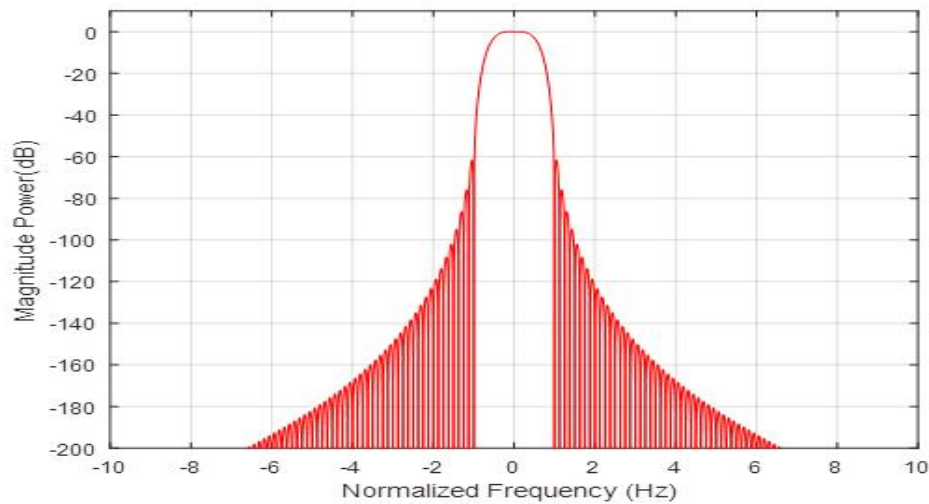


Figure 3: Frequency Impulse Response of PHYDYAS Filter.

A decaying trend could be seen in Figure (3) which is the basis for the filter choice. Parallel filters at the transmitter which made up the synthesis filter bank (SFB) at the filters are mapped with the analysis filter bank (AFB) at the receiver.

OQAM Modulation of the FBMC Signal and Matrix Representation of the Modulated Data Symbols.

In modulating the FBMC signal, the real and imaginary components of the complex signal were generated and then successively transmitted between a half symbol delay. With the set-up parameters of Table 3, IFFT of size 1024 was implemented on the FBMC symbols of equation (7).

The reason for representing the OQAM-modulated FBMC data symbols in matrix format is to ease the computations involved by getting rid of unnecessary calculations. Maintaining the established set-up assumptions, the OQAM-modulated prototype pulse $p_{l,k}(t)$, and the complex transmit symbol $d_{l,k}$, at subcarrier position l and multicarrier position k of equation (5) were written as basis pulse vectors $P_{l,k} \in \mathbb{C}^{N \times 1}$ and $D_{l,k} \in \mathbb{C}^{LK \times 1}$. A stack of all the basis pulses is $P_{l,k} \in \mathbb{C}^{N \times LK}$ which transforms into the following:

$$P = \begin{pmatrix} P_{1,1} & \cdots & P_{1,LK} \\ \vdots & \ddots & \vdots \\ P_{n,1} & \cdots & P_{n,LK} \end{pmatrix} \quad (15)$$

$$P = (P_{1,1} \cdots P_{n,1}, P_{1,LK} \cdots P_{n,LK}) \quad (16)$$

A stack of all the transmit symbols is $D_{l,k} \in \mathbb{C}^{LK \times N}$ which translates to the following:

$$D = \begin{pmatrix} d_{1,1} & \cdots & d_{1,n} \\ \vdots & \ddots & \vdots \\ d_{lk,1} & \cdots & d_{lk,n} \end{pmatrix} \quad (17)$$

$$D = (d_{1,1} \cdots d_{lk,1}, d_{1,n} \cdots d_{lk,n}) \quad (18)$$

The modulated transmit signal of equation (5) is matrix format is now expressed as follows:

$$S = PD \quad (19)$$

The received basis pulse $q_{l,k}$ at subcarrier position l and multicarrier position k in a basis pulse vector is $Q_{l,k} \in \mathbb{C}^{N \times 1}$ and a stack of all the received basis pulses is $Q_{l,k} \in \mathbb{C}^{N \times LK}$ which transforms into the following:

$$Q = \begin{pmatrix} q_{11} & \cdots & q_{1,n} \\ \vdots & \ddots & \vdots \\ q_{lk,1} & \cdots & q_{lk,n} \end{pmatrix} \quad (20)$$

$$Q = (q_{1,1} \cdots q_{lk,1}, q_{1,n} \cdots q_{lk,n}) \quad (21)$$

The sampled received signal $r(t)$ at time position v , met with a delay \dagger such that its impulse response h was modeled as time-variant convolution matrix $H \in \mathbb{C}^{N \times N}$. The total received signal $r(t)$ when piled as a vector signal is as follows:

$$r = HQD \quad (22)$$

While a stack of the received symbols is thus:

$$y = Q^H r \quad (23)$$

where Q^H is the Hermitian of Q , whose conjugate of its complex entries is equal to the transpose of its complex conjugate.

$$y = Q^H HQD \quad (24)$$

In an additive white Gaussian (AWGN) channel where P equals Q , and in the presence of Gaussian distributed noise but negligible channel induced interference, the received symbol is as follows:

$$y = Q^H HPD + n \quad (25)$$

where n is the Gaussian distributed noise.

Restoring (Bi)-Orthogonality by Hadamard Scheme

Hadamard coding scheme was employed to the modulated transmit signal of equation (25) to restore the complex orthogonality of the FBMC-OQAM system. Assuming an additive white Gaussian noise channel, the impulse response of the system is an identity matrix as follows:

$$H = I_n \quad (26)$$

Equation (25) thus becomes the following:

$$y = Q^H PD + n \quad (27)$$

The complex valued transmit-data symbols of equation (18) were pre-coded with a Hadamard matrix C written as a pulse vector

$C_{l,k} \in \mathbb{C}^{1 \times LK}$ which was stacked as follows:

$$C = \begin{pmatrix} c_{1,1} & \cdots & c_{1,LK} \\ \vdots & \ddots & \vdots \\ c_{N,1} & \cdots & c_{N,LK} \end{pmatrix} \quad (28)$$

$$C = (c_{1,1} \cdots c_{N,1}, c_{1,LK} \cdots c_{N,LK}) \quad (29)$$

The stack of the coded complex transmit symbols D of equation (25) is translated to the following:

(3.14)

$$D = C D^c$$

The received coded symbol $y^c \in \mathbb{C}^{1 \times LK}$ was obtained by projecting the stacked impulse response of the Hadamard matrix into the received symbols y as follows:

$$y^c = C^H y$$

$$y^c = C^H Q^H P D + n$$

$$y^c = C^H Q^H P C D^c + n$$

With P equals Q in AWGN channel, the received coded symbol, y^c , becomes the following:

$$y^c = C^H Q^H Q C D^c + n \quad (34)$$

The terms $C^H Q^H Q C$ constitute an identity matrix of size LK which establishes the orthogonality of the system as given in equation (8) [16]. The orthogonality was checked by plotting a diagonally plot of the subcarrier position against the multicarrier position of the complex data symbols which ascertains orthogonality of the data symbols. The orthogonality plot is given in Figure 4.

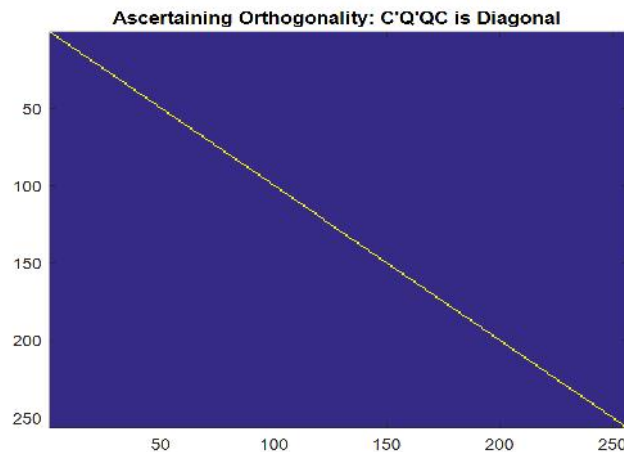


Figure 4: Restored Orthogonality Ascertained by diagonal $C^H Q^H Q C$.

CONCLUSION

The congestion coupled with underutilization of the available radio spectrum in the sub-six Giga Hertz scarcity of radio spectrum in wireless communication necessitates the need for spectral and bandwidth channel efficient schemes that will ensure the optimal utilization, especially in the next generation wireless communications systems. By employing Hadamard coding scheme on OQAM-modulated FBMC, orthogonality in its imaginary field was restored to have bi-orthogonal carrier signals. As such, assuming zero channel impairments,

the spectral efficiency and bandwidth channel capacity was doubled.

REFERENCES

- [1] J. Abdoli, M. Jia, and J. Ma, "Filtered OFDM: A new waveform for future wireless systems," in *Signal Processing Advances in Wireless Communications (SPAWC), 2015 IEEE 16th International Workshop on*, 2015, pp. 66-70.
- [2] R. Nissel, J. Blumenstein, and M. Rupp, "Block frequency spreading: A method for low-complexity MIMO in FBMC-OQAM," in *Signal Processing*



- Advances in Wireless Communications (SPAWC), 2017 IEEE 18th International Workshop on*, 2017, pp. 1-5.
- [3] P. Siohan, C. Siclet, and N. Lacaille, "Analysis and design of OFDM/OQAM systems based on filterbank theory," *IEEE transactions on signal processing*, vol. 50, pp. 1170-1183, 2002.
- [4] A. Farhang, N. Marchetti, L. E. Doyle, and B. Farhang-Boroujeny, "Filter bank multicarrier for massive MIMO," *Signal Processing for G*, vol. 5, pp. 67-89, 2014.
- [5] V. Moles-Cases, A. A. Zaidi, X. Chen, T. J. Oechtering, and R. Baldemair, "A comparison of OFDM, QAM-FBMC, and OQAM-FBMC waveforms subject to phase noise," in *Communications (ICC), 2017 IEEE International Conference on*, 2017, pp. 1-6.
- [6] M. H. Halmi, M. Abdellatif, and N. Nooridin, "Orthogonal space-time block codes for large MIMO systems," in *Communications, Management and Telecommunications (ComManTel), 2015 International Conference on*, 2015, pp. 78-82.
- [7] A. Zafar, "Filter bank based multicarrier systems for future wireless networks," University of Surrey, 2018.
- [8] S. Chaudhary and A. Patil, "Performance analysis of mimo-space time block coding with different modulation techniques," *ICTACT Journal on communication technology*, vol. 3, 2012.
- [9] M. Ja'afar, S. Sani, and A. Tekanyi, "Application of Filter Bank Multicarrier Offset Quadrature Amplitude Modulation to Large MIMO Systems: A Review," in *2019 2nd International Conference of the IEEE Nigeria Computer Chapter (NigeriaComputConf)*, 2019, pp. 1-8.
- [10] R. Nissel and M. Rupp, "Enabling Low-Complexity MIMO in FBMC-OQAM," in *GLOBECOM Workshops*, 2016, pp. 1-6.
- [11] N. Malla and H. D. G. Joshi, "Study and Analysis of Carrier Frequency Offset (CFO) in OFDM," 2014.
- [12] R. Nissel, E. Zochmann, and M. Rupp, "On the influence of doubly-selectivity in pilot-aided channel estimation for FBMC-OQAM," in *Vehicular Technology Conference (VTC Spring), 2017 IEEE 85th*, 2017, pp. 1-5.
- [13] F. Rottenberg, "FBMC-OQAM transceivers for wireless and optical fiber communications," UCL-Université Catholique de Louvain, 2018.
- [14] M. Cheraghchi, V. Guruswami, and A. Velingker, "Restricted isometry of Fourier matrices and list decodability of random linear codes," *SIAM Journal on Computing*, vol. 42, pp. 1888-1914, 2013.
- [15] K. Dostert, *Powerline communications*: Prentice Hall PTR, 2001.
- [16] M. Malek, "Hadamard Codes," *California State University*, vol. 112, 2015.
- [17] A. Viholainen, T. Ihalainen, T. H. Stitz, M. Renfors, and M. Bellanger, "Prototype filter design for filter bank based multicarrier transmission," in *2009 17th European Signal Processing Conference*, 2009, pp. 1359-1363.
- [18] R. Nissel, S. Schwarz, and M. Rupp, "Filter bank multicarrier modulation schemes for future mobile communications," *IEEE Journal on Selected Areas in Communications*, vol. 35, pp. 1768-1782, 2017.